# Caloric Restriction Mimetics Enhance Anticancer Immunosurveillance

Federico Pietrocola, Jonathan Pol, Erika Vacchelli, Shuan Rao, David p. Enot, Elisa e. Baracco, Sarah Levesque, Francesca Castoldi, Nicolas Jacquelot, Takahiro Yamazaki, et al.

Published in final edited form as:

*Cancer Cell*. 2016 July 11; 30(1): 147–160. doi:10.1016/j.ccell.2016.05.016.

# Caloric Restriction Mimetics Enhance Anticancer Immunosurveillance

**Federico Pietrocola**[1,2,3,23], **Jonathan Pol**[1,2,3,5,23], **Erika Vacchelli**[1,2,3], **Shuan Rao**[6], **David P. Enot**[1,7], **Elisa E. Baracco**[1,2,3,4], **Sarah Levesque**[1,2,3,4], **Francesca Castoldi**[1,2,3,4,8], **Nicolas Jacquelot**[1,4,9,10], **Takahiro Yamazaki**[1,4,9,10], **Laura Senovilla**[1,2,3,5], **Guillermo Marino**[1,2,3], **Fernando Aranda**[1,2,3], **Sylvère Durand**[1,7], **Valentina Sica**[1,2,3,4], **Alexis Chery**[1,7], **Sylvie Lachkar**[1,2,3,4], **Verena Sigl**[6], **Norma Bloy**[1,2,3,4], **Aitziber Buque**[1,2,3,4], **Simonetta Falzoni**[11], **Bernhard Ryffel**[12,13], **Lionel Apetoh**[14,15,16], **Francesco Di Virgilio**[11], **Frank Madeo**[17,18], **Maria Chiara Maiuri**[1,2,3,4], **Laurence Zitvogel**[1,4,9,10], **Beth Levine**[19], **Josef M. Penninger**[6,24], and **Guido Kroemer**[1,2,3,5,7,20,21,22,24,*]

[1]Gustave Roussy Cancer Campus, 94800 Villejuif, France

[2]INSERM, U1138, 75006 Paris, France

[3]Equipe 11 labellisée par la Ligue Nationale contre le Cancer, Centre de Recherche des Cordeliers, 75006 Paris, France

[4]Université Paris-Sud/Paris-Saclay, Faculté de Médecine, 94276 Kremlin-Bicetre, France

[5]Université Paris Descartes/Paris V, Sorbonne Paris Cité, 75006 Paris, France

[6]Institute for Molecular Biotechnology of the Austrian Academy of Sciences, 1030 Vienna, Austria

[7]Metabolomics and Cell Biology Platforms, Gustave Roussy Cancer Campus, 94800 Villejuif, France

[8]Sotio a.c, 17000 Prague, Czech Republic

[9]INSERM U1015, Gustave Roussy Cancer Campus, 94800 Villejuif, France

[10]Center of Clinical Investigations in Biotherapies of Cancer (CICBT) 1428, 94800 Villejuif, France

[11]Department of Morphology, Surgery and Experimental Medicine University of Ferrara, 44121 Ferrara, Italy

[12]UMR7355, CNRS and University, 45067 Orléans, France

[13]Institute of Infectious Disease and Molecular Medicine, University of Cape Town, 7925 Cape Town, South Africa

[*]Correspondence: kroemer@orange.fr.
[23]Co-first author
[24]Co-senior author

Supplemental Information: Supplemental Information includes Supplemental Experimental Procedures, seven figures, and three tables and can be found with this article online at http://dx.doi.org/10.1016/j.ccell.2016.05.016.

**Author Contributions**: F.P., J.P., E.V., S.R., E.E.B., S.V., F.C., N.J., T.Y., L.S., G.M., F.A., V.S., S.L, V.S., N.B., A.B., and S.F. performed the experiments. S.D., D.P.E., and A.C., performed mass spectrometry and data analysis. B.R., and L.A. provided DEREG mice. F.D.V., F.M.C., and M.C.M., helped to design the study. F.P., J.P., S.R., L.Z., B.L, J.M.P., and G.K. designed the study, analyzed the data, and wrote the paper.

[14]INSERM, U866, 21078 Dijon, France

[15]Faculté de Médecine, Université de Bourgogne, 21078 Dijon, France

[16]Centre Georges François Leclerc, 21000 Dijon, France

[17]Institute of Molecular Biosciences, NAWI Graz, University of Graz, Humboldtstraβe 50, 8010 Graz, Austria

[18]BioTechMed-Graz, Humboldtstraβe 50, 8010 Graz, Austria

[19]Department of Internal Medicine, Center for Autophagy Research, Howard Hughes Medical Institute, University of Texas Southwestern Medical Center, Dallas, TX 73590, USA

[20]Pôle de Biologie, Hôpital Européen Georges Pompidou, AP-HP, 75015 Paris, France

[21]Department of Women's and Children's Health, Karolinska Institute, Karolinska University Hospital, Stockholm, Sweden

[22]INSERM U1138, Centre de Recherche des Cordeliers, 75006 Paris, France

## Summary

Caloric restriction mimetics (CRMs) mimic the biochemical effects of nutrient deprivation by reducing lysine acetylation of cellular proteins, thus triggering autophagy. Treatment with the CRM hydroxycitrate, an inhibitor of ATP citrate lyase, induced the depletion of regulatory T cells (which dampen anticancer immunity) from autophagy-competent, but not autophagy-deficient, mutant KRAS-induced lung cancers in mice, thereby improving anticancer immunosurveillance and reducing tumor mass. Short-term fasting or treatment with several chemically unrelated autophagy-inducing CRMs, including hydroxycitrate and spermidine, improved the inhibition of tumor growth by chemotherapy in vivo. This effect was only observed for autophagy-competent tumors, depended on the presence of T lymphocytes, and was accompanied by the depletion of regulatory T cells from the tumor bed.

## In Brief

Pietrocola et al. show that short-term fasting or autophagy-inducing caloric restriction mimetics, such as hydroxycitrate and spermidine, improves the antitumor efficacy of chemotherapy in vivo. The effect is specific for autophagy-competent tumors and depends on regulatory T cell depletion from the tumor bed.

## Introduction

Accumulating evidence suggests that the long-term success of antineoplastic therapies is largely determined by their capacity to reinstate anticancer immunosurveillance (Galluzzi et al., 2015a). This does not only apply to so-called immunotherapies but may also hold true for conventional chemo-and radiotherapy. In particular, chemotherapies with anthracyclines or oxaliplatin can stimulate immunogenic cell death (ICD), thus converting dying tumor cells into a therapeutic vaccine that elicits a potent immune response mediated by cytotoxic T lymphocytes against residual tumor cells (Kepp et al., 2014).

Chemotherapeutic agents that stimulate ICD have the particularity to cause premortem stress at the level of the ER (which favors the exposure of calreticulin as an “eat me” signal on the surface of stressed/dying cells) (Obeid et al., 2007) and to stimulate macroautophagy (which we refer to as “autophagy”), a phenomenon whereby portions of the cytoplasm are sequestered in autophagosomes, which subsequently fuse with lysosomes for the degradation of autophagic cargo by lysosomal hydrolases (Jiang and Mizushima, 2014; Mizushima et al., 2008). In normal cells, autophagy constitutes a barrier against malignant transformation. Accordingly, many oncosuppressor proteins promote, and several oncoproteins suppress, autophagy (Galluzzi et al., 2015b). In neoplastic cells, however, autophagy may facilitate the adaptation to cell-intrinsic and -extrinsic stress, thus favoring tumor progression (White, 2015). Thus, depending on the context, autophagy may antagonize oncogenesis or facilitate malignant progression (Galluzzi et al., 2015b), spurring interest in the development of pharmacological modulators of autophagy (Levine et al., 2015; Rubinsztein et al., 2012).

Premortem autophagy is not essential for chemotherapy-elicited cancer cell death to occur (Guo et al., 2013), but is indispensable for ICD, because autophagy is required for the release of ATP into the extracellular space where ATP serves as a chemotactic factor to attract antigen-presenting cells into the vicinity of dying cells (Ma et al., 2013; Michaud et al., 2011). This effect is achieved by the capacity of extracellular ATP to act on purinergic receptors (such as P2YR2 receptors) present on the surface of immature dendritic cell precursors (Ma et al., 2013). The suppression of autophagy in tumor cells or the blockade of purinergic receptors on immune cells abolishes the capacity of chemotherapy to stimulate the invasion of tumors by antigen-presenting cells (Ma et al., 2013). When autophagy is disabled, tumor cells overexpress CD39, an ecto-enzyme that degrades extracellular ATP into immunosuppressive adenosine, hence attracting regulatory T cells (Tregs) expressing adenosinergic receptors into the tumor bed (Rao et al., 2014). After treatment with ICD inducers, autophagy-deficient or CD39-over-expressing tumor cells fail to elicit a therapeutic immune response, which facilitates resistance against conventional cancer treatments (Ko et al., 2014; Michaud et al., 2011).

One particularly efficient strategy for increasing the efficacy of therapy in mouse models of cancer consists in combining chemotherapy with a regimen of acute (48 hr) starvation (Lee et al., 2012). Of note, nutrient starvation for 24–48 hr is also one of the most efficient ways to elicit autophagy in most cells of the organism (Mizushima et al., 2004). Based on these premises, we investigated the hypothesis that starvation and pharmacological autophagy induction might stimulate anticancer immunosurveillance. We therefore investigated the capacity of several non-immunosuppressive autophagy inducers that mimic the metabolic effects of starvation, so-called caloric restriction mimetics (CRMs) (Madeo et al., 2014), to improve the therapeutic outcome of immunogenic chemotherapies and enhance immunosurveillance.

## Results

### Starvation Improves Chemotherapy via T Cells and Autophagy

Starvation is the most physiological way of inducing autophagy in most organs of mice (Mizushima et al., 2004). The antineoplastic effects of chemotherapy are known to be improved by fasting (Lee et al., 2012), although the underlying mechanisms have been elusive. Mitoxantrone (MTX) or oxaliplatin (OX) caused a reduction in the growth of murine MCA205 fibrosarcoma established in immunocompetent wild-type (WT) mice, a therapeutic effect that was markedly improved when chemotherapy was combined with starvation for 48 hr (starting 24 hr after initiation of fasting). Importantly, these effects were entirely dependent on the cellular immune system because both chemotherapy alone (with MTX or OX) and chemotherapy plus starvation were unable to control tumors growing in athymic *nu*/*nu* mice, which lack T lymphocytes (Figures 1A and 1B; Tables S1 and S2). Moreover, the inhibitory effect of starvation on tumor growth was lost in cancers that had been rendered autophagy deficient upon the knockdown of the essential autophagy-related gene *Atg5* (Figures 1C and 1D). We conclude from these results that starvation can enhance chemotherapy-induced immunosurveillance in an autophagy-dependent fashion.

### Hydroxycitrate Stimulates AutophagyInVitro and In Vivo

The biochemical effects of starvation can be mimicked by so-called CRMs, which are non-toxic pharmacological agents or natural compounds that reduce cellular protein acetylation, thereby increasing autophagic flux (Madeo et al., 2014). One compound that falls into this definition is hydroxycitrate (HC) (Marino et al., 2014), an over-the-counter weight loss agent that has been evaluated in clinical trials as an anti-obesity agent (Onakpoya et al., 2011). HC acts as a competitive inhibitor of the ATP citrate lyase (ACLY), an enzyme that generates cytosolic acetyl coenzyme A (AcCoA) (Onakpoya et al., 2011). HC (but not citrate) and two additional, chemically unrelated ACLY inhibitors (SB-204990, BMS-303141) stimulated autophagic flux in cultured cancer cells, as indicated by the autophagy-associated conversion of LC3 I to LC3 II and the distribution of initially diffuse GFP-LC3 fusion protein to cytoplasmic puncta (Figures S1A and S1B), even in the presence of bafilomycin A1 (which blocks the lysosomal removal of LC3 II- or GFP-LC3-containing autophagosomes) (Klionsky et al., 2012). HC-induced autophagy was suppressed by microinjection of AcCoA (Figure 2A) but not by supplementation of mevalonate, which only suppresses statin-induced autophagy (Figure S1C). In line with these findings, HC induced autophagy irrespective of hydroxymethylglutaryl CoA reductase (HMGCR) or acetyl CoA carboxylase (ACC) expression, ruling out the possibility that HC-induced autophagy was due to the inhibition of lipid or sterol biosynthesis (Figure S1D). HC reduced cytoplasmic protein acetylation, as determined by immunofluorescence staining with an antibody reacting with N-ε-acetyl lysine residues (Figure 2B). Two intraperitoneal injections of HC on consecutive days were similarly efficient as a starvation period of 48 hr (during which mice had ad libitum access to water, but not to food) at inducing the autophagy-related conversion of LC3 I to LC3 II in mouse tissues in vivo (Figure 2C), with efficiency similar to that of well-established CRMs such as the sirtuin-1 activator resveratrol and the E1A binding protein p300 (EP300) acetyltransferase inhibitors spermidine and C646 (Marino et al., 2014; Morselli et al., 2011). However, compared with 48 hr starvation, HC

induced a virtually negligible weight loss (Figure 2D). Starvation and a diverse array of CRMs including HC caused largely convergent perturbations of the metabolome in vivo, in multiple distinct organs (Figures 2E, 2F, and S2; Table S3), as they reduced the bioavailability of circulating insulin growth factor 1 (IGF-1) levels (with a corresponding increase in inhibitory IGF-1 binding protein 1, IGFBP1) (Figure 2G). Hence, HC and other CRMs induce similar biochemical changes in mice including autophagy in vivo, as does starvation, yet fail to cause a major weight loss.

## Hydroxycitrate Improves Chemotherapy in a T Cell-Dependent Fashion

Two injections of HC on consecutive days into mice fed ad libitum induced autophagy as efficiently as did starvation, both in the liver (Figure 2C) and tumors implanted in the flank (Figure S3A). Daily administration of HC (starting 1 day before chemotherapy) also improved the therapeutic outcome in MCA205 fibrosarcomas (Figures 3A and 3B), CT26 colorectal cancers (Figure S3B), and TC-1 non-small cell lung cancers (Figure S3C) established in immunocompetent mice that were treated with MTX (Figures 3A, S3B, and S3C) or OX (Figure 3B), yet failed to improve the efficacy of *cis*-diamminedichloroplatinum(II) (CDDP, also known as cisplatin), a chemotherapeutic agent that does not elicit ICD (Figure S3D). The combination of HC and MTX was more efficient than single agents in reducing the growth of primary sex-hormone-driven breast cancer (left panels in Figures 3C–3E). This tumor growth-reducing and survival-extending effect was lost when the animals were rendered immunodeficient by injecting antibodies that deplete $CD8^+$ (but not $CD4^+$) T lymphocytes (right panels in Figures 3C–3E). Similarly, depletion of $CD8^+$ T cells was sufficient to abolish MCA205 tumor growth reduction by MTX plus HC (Figures S4A and S4B). The MTX-HC combination was particularly efficient in increasing the frequency of proliferating ($Ki67^+$) $CD8^+ICOS^+$ cells within the tumor bed (Figure S4C). Moreover, in the TC1 model (which expresses the HPV-E7 antigen), HC was able to increase the frequency of tumor antigen-specific $CD8^+$ T cells in the draining lymph node induced by therapeutic vaccination (Figure S4D). Hence, the capacity of HC to improve the outcome of chemotherapy depended on the elicitation of an adaptive cellular immune response in several distinct tumor models, namely fibrosarcomas, mammary carcinomas, and non-small cell lung cancers.

## Autophagy Induction Improves Chemotherapy in an Immune-Dependent Fashion

The specific ACLY inhibitor SB-204990 was as efficient as HC in inducing autophagy in vivo (Figure S3A) and in improving the antineoplastic efficacy of MTX (Figure 4A), supporting the contention that HC mediates antineoplastic effects via an on-target mechanism. Importantly, HC could be replaced by other, chemically unrelated CRMs that act through a variety of distinct molecular mechanisms yet all cause protein deacetylation, including spermidine (a natural compound that inhibits several acetyltransferases including EP300) (Eisenberg et al., 2009; Pietrocola et al., 2015) (Figure 4B) and C646 (a synthetic EP300 inhibitor) (Figure 4C), both of which also induced autophagy within the tumors (Figure S3A). Moreover, treatment with the sirtuin-1 activator resveratrol enhanced the therapeutic effects of anthracyclines (Figures S3A and 4D), as did intraperitoneal injection of Tt-B (Figures 4E, S3A, and S5A–S5C), a cell-permeable peptide that has been designed to activate the pro-autophagic Beclin 1 protein complex (Shoji-Kawata et al., 2013).

Importantly, all combination regimens (MTX + SB, MTX + spermidine, MTX + C646, MTX + resveratrol, MTX + Tt-B) showed a more prominent anti-cancer activity compared with single-agent administration yet failed when the cellular immune system was compromised due to the *nu*/*nu* mutation (Figures 4A–4E). These results suggest that pharmacological autophagy induction may enhance the efficacy of anticancer therapies by boosting a T cell-mediated immune response.

## Requirement of Autophagy for Hydroxycitrate-Improved Chemotherapy

The combination of HC and MTX induced a higher level of autophagy-dependent release of ATP from cultured tumor cells in vitro than either agent alone (Figures 5A and S6A). Similarly, the combination of MTX plus HC was particularly efficient in inducing extracellular ATP accumulation (which can be measured in vivo by tethering a luciferase construct on the surface of tumor cells) (Pellegatti et al., 2008) (Figure 5B). This effect was only found in autophagy-competent tumors, not in tumors in which *Atg5* had been depleted by transfection with a construct encoding a specific short hairpin RNA (shRNA) (Figures 5A and 5B). Only autophagy-competent tumors (which were transfected with a control shRNA) exhibited a significant therapeutic response to HC plus MTX, whereas cancers depleted of *Atg5* were resistant to the adjuvant therapeutic effect of HC (Figure 5C). Similarly, cancers engineered to express the ecto-ATPase CD39 (which converts extracellular ATP into ADP and AMP) failed to respond to the combination of chemotherapy + MTX (Figure 5C), underscoring the importance of extracellular ATP for the response. Injection of an antibody specific for CD73 (an ecto-enzyme that converts AMP into immunosuppressive adenosine) (Stagg et al., 2011; Loi et al., 2013a) improved the efficacy of MTX as much as did HC, yet failed to mediate the additive effect with HC (Figure S6B). This epistatic analysis suggests that HC indeed acts through the modulation of extracellular ATP metabolism. HC-induced autophagy could be inhibited by injection of recombinant IGF-1 protein in vitro (Figures 5D and 5E) andin vivo (Figures 5F and 5G), amaneuver that abolished tumor growth reduction by HC (Figure 5H). Thus, similar to starvation (Figure 1D), HC-mediated enhancement of the chemotherapeutic effect relies on the induction of autophagy in tumor cells.

## Hydroxycitrate-Improved Chemotherapy Is Mediated by Treg Depletion

The combination of MTX and HC (but neither of these two agents alone) markedly reduced the frequency of tumor-infiltrating $CD4^+CD25^+Foxp3^+$ Tregs (Figures 6A and 6B), and this Treg-depleting effect was abolished when animals were treated with an autophagy-inhibitory dose of recombinant IGF-1 protein (Figure 6B). Direct inhibition of autophagy in tumor cells by knockdown of *Atg5* or transfection-enforced expression of the ecto-ATPase CD39 also prevented the depletion of Tregs by MTX and HC (Figures 6C and 6D), suggesting that autophagy in, and consequent ATP release from, cancer cells are required for the reduction in Treg infiltration. Depletion of Tregs using an antibody recognizing FR4 (Yamaguchi et al., 2007; McNally et al., 2011), or by diphtheria toxin (DT) administration into DEREG mice expressing the DT receptor under the control of the *Foxp3* promoter (Lahl et al., 2007; Teng et al., 2010), controlled or caused the regression of MCA205 fibrosarcomas (Figures 6E and 6F) and established TC1 lung cancers (Figure S6C). Importantly, epistatic analyses revealed that HC administration failed to further improve the anticancer effects of Treg

depletion, supporting the contention that HC increases the efficacy of chemotherapy by reducing Treg infiltration into tumors.

### Hydroxycitrate Stimulates Immunosurveillance Against KRas-Induced Lung Cancers

Caloric restriction is known to limit the growth of *KRas*$^{G12D}$-induced lung cancers provoked by delivering a Cre recombinase-encoding adenovirus (Ad-Cre) into the lungs of mice bearing a Lox-Stop-Lox-*KRas*$^{G12D}$ transgene (Kalaany and Sabatini, 2009). Administration of HC induced autophagy in *KRas*-induced lung adenocarcinomas, but only if they expressed at least one normal *Atg5* allele (*Atg5*$^{fl/+}$). When both alleles of *Atg5* were floxed (*Atg5*$^{fl/fl}$), the resulting Atg5-deficient tumor cells were unable to generate LC3 dots in response to HC (Figures S7A and S7B). HC also reduced the number and size of Ad-Cre-induced tumor lesions in *KRas*;*Atg5*$^{fl/+}$ but not *KRas*;*Atg5*$^{fl/fl}$ mice (Figures 7A and 7B). Paralleling its anticancer effects, HC reduced the density of tumor-infiltrating Foxp3$^{+}$ Treg cells (Figure 7C), with a consequent altered percentage of Foxp3$^{+}$ (Figure S7F) among CD3$^{+}$ lymphocytes (Figures S7D and S7E) in *KRas*;*Atg5*$^{fl/+}$ tumors only (Figure 7D). Depletion of Tregs by antibodies recognizing two Treg surface antigens, namely CD25 or FR4, also reduced *KRas*-induced oncogenesis, and this effect could not be further improved by simultaneous treatment with HC (Figure 7E). HC failed to reduce the growth of lung cancers evolving in *Rag2*$^{-/-}$ mice, which lack T and B lymphocytes (Figure S7C), or mice that expressed transgenic CD39 in the tumors (Figure 7F). These results indicate that HC-mediated stimulation of autophagy within cancer cells causes Treg depletion, which in turn improves immunosurveillance against *KRas*-induced neoplasia.

## Discussion

Immunogenic chemotherapy with anthracyclines or oxaliplatin is known to stimulate an anticancer immune response that may be largely responsible for the long-term effects of successful treatment regimens, both in animal models (Zitvogel et al., 2013) and in patients with mammary carcinoma (Sistigu et al., 2014) and colorectal cancer (Bindea et al., 2013; Tesniere et al., 2010). One of the requisites of immunogenic chemotherapy is the induction of autophagy (Michaud et al., 2011), a process that allows for optimal lysosomal exocytosis of ATP from dying tumor cells (Martins et al., 2014) and avoids the upregulation of the immunosuppressive ecto-ATPase CD39(Rao et al., 2014). Autophagy occurring in malignant cells is indeed essential for anticancer chemotherapy and radiotherapy to work, meaning that defective autophagy due to the reduced expression of essential *Atg* genes largely compromises therapeutic efficacy (Ko et al., 2014; Michaud et al., 2011, 2014). As reported here, artificial overstimulation of autophagy by starvation, CRMs, or therapeutic agents that have been specifically designed to trigger this process (Levine and June, 2013) can improve the immune-dependent antineoplastic effects of chemotherapy. Indeed, autophagy occurring within cancer cells was obligatory for the therapeutic efficacy of CRMs such as HC, likely because autophagy-deficient cells escape from natural and therapy-induced immunosurveillance as they attract Tregs into the tumor bed (Ma et al., 2013; Michaud et al., 2011; Rao et al., 2014; Uhl et al., 2009). In addition, pharmacological autophagy induction could improve immunosurveillance in an oncogene-induced model of lung cancer, and this effect again involved the depletion of tumor-infiltrating Tregs. As a limitation of our study,

however, we must point out that enhanced ATP release coupled to Treg depletion was defined as the mechanism of the anticancer action of HC in only two transplantable tumor models and one oncogene-induced cancer. Therefore, further studies are required to define the mechanistic details through which CRMs exert their beneficial action on anticancer immunosurveillance.

Circumstantial and epidemiological evidence indicates that overfeeding and obesity constitute negative prognostic factors with regard to the incidence, progression, and therapeutic response of several human malignancies (Casagrande et al., 2014; Gilbert and Slingerland, 2013; Makarem et al., 2013). In contrast, caloric restriction and fasting have been related to positive therapeutic outcome, both in animal models (Kalaany and Sabatini, 2009; Lee et al., 2012) and in humans subjected to voluntary fasting (Lee and Longo, 2011) or bariatric surgery (Tee et al., 2013). Here, we report that a 48 hr starvation period (which in mice causes a dramatic, yet recoverable weight loss of ~20%) can improve the efficacy of chemotherapy via an immunological mechanism that involves a reduction in the intra-tumoral infiltration by Tregs. Starvation cycles reportedly trigger the rejuvenation of immune-relevant hematopoietic stem cells, suggesting additional immunostimulatory effects that might contribute to the improved immunosurveillance (Cheng et al., 2014). Our present data indicate that starvation might be replaced by a special diet or by natural compounds that mimic starvation with regard to the induction of metabolic alterations and autophagic responses in vivo.

Among the agents that we describe here as CRMs with positive effects on anticancer immunosurveillance, several have a rather favorable toxicological profile. Chronic treatment with spermidine or rapamycin even extends the health and life spans of mice (Harrison et al., 2009; Kibe et al., 2014; Strong etal., 2008), suggesting that at least some CRMs might have a favorable risk/benefit profile. Furthermore, HC has been evaluated in clinical trials as a weight-reduction agent in obese patients, without major side effects (Chuah et al., 2012; Onakpoya et al., 2011). Future work is required to understand which particular CRM (or CRM combination) will be optimally suitable for cancer-preventive or therapeutic improvement of immunosurveillance.

## Experimental Procedures

### Mouse Strains and Housing

Mice were maintained in specific pathogen-free conditions in a temperature-controlled environment with 12-hr light/12-hr dark cycles and received food and water ad libitum (unless noted otherwise). Animal experiments were in compliance with the EU Directive 63/2010, and protocols 2012_069 and 2015_026_1114 were approved by the Ethical Committee of the Gustave Roussy Campus Cancer (CEEA IRCIV/IGR no. 26, registered at the French Ministry of Research). Six-to 7-week-old female WT C57Bl/6, BALB/c, and nude athymic (*nu*/*nu*) mice were obtained from Harlan France. All mouse experiments were randomized and blinded, and sample sizes were calculated to detect a statistically significant effect.

*Atg5*$^{fl/fl}$ mice were kindly provided by Dr. Noboru Mizushima. *LSL-K-rasG12D*;*Atg5*$^{fl/fl}$ mice were obtained as described by Rao et al. (2014). The CD39 transgenic mice were kindly provided by Dr. Peter Cowan. CD39 transgenic mice were crossed with *LSL-K-rasG12D*;*Atg5*$^{fl/fl}$ mice to obtain *LSL-K-rasG12D*;*Atg5*$^{fl/fl}$;*CD39*$^{+}$ mice. In all experiments, only littermate mice were used as controls. All mice were maintained according to the ethical animal license protocol complying with the Austrian and European legislation. All experiments were approved by Bundesministerium for Wissenschaft und Forschung, Austria (BMWF-66.015/0013-II/3b/2012).

Depletion of REGulatory T cells (DEREG) transgenic mice (Lahl et al., 2007) were kindly provided by Drs. Bernard Ryffel and Lionel Apetoh.

## Mouse Experiments and Tissue Processing

For tumor growth experiments, $3\times10^5$ WT MCA205, TC-1, or CT26 cells were inoculated subcutaneously (near the thigh) into WT or *nu/nu* C57BL/6 (H-2b) mice, and tumor surface (longest dimension 3 perpendicular dimension) was routinely monitored using a common caliper. When the tumor surface reached 25–35 $mm^2$, mice were treated intraperitoneally either with 5.17 mg/kg mitoxantrone (MTX) in 100 μl of PBS, 10 mg/kg oxaliplatin (OX) in 100 μl of PBS, 10 mg/kg CDDP, or an equivalent volume of PBS, alone or in combination with daily administration of 900 mg/kg hydroxycitrate (HC) in drinking water; or 30 mg/kg SB204990 (SB), 25 mg/kg resveratrol (Resv), 10 mg/kg C646, 50 mg/kg spermidine (Spd), 5 mg/kg rapamycin (Rapa). Tat-Beclin-1 (Tt-B) peptide (17) or Tat-Beclin-1 (Tt-S) peptide (17S) were administered intraperitoneally at a dose of 15 mg/kg in 100 μl of PBS three times per week. Tt-B (17) is an optimized derivative of the previously published autophagy-inducing Tt-B peptide (YGRKKRRQRRC-GGVWNATF HIWHD) and contains the sequence YGRKKRRQRRC-GGVWNATFHIWHD. Tat-Beclin 1 mutant (17S) (YGRKKRRQRRC-GG-VSNATFHIWHD) contains a serine substitution mutation at the amino acid position corresponding to 270 of full-length Beclin 1 that abolishes its autophagy activity. Both peptides were synthesized by the Protein Technology Chemistry Core at UT Southwestern Medical Center. For antibody-mediated depletion experiments, 10 μg of monoclonal anti-FR4 (intravenously), and 100 μg of monoclonal anti-CD73, anti-CD4, or anti-CD8 antibodies (intraperitoneally) were injected 2 days before, on the same day, and 1 week after chemotherapy. 200 mg/kg intraperitoneal IGF-1 recombinant protein was administered daily.

For starvation experiments, mice underwent 48 hr fasting followed by intraperitoneal injection of chemotherapeutics.

For autophagy induction studies, after CRMs administration on two consecutive days, mice were euthanized and tissues were snap-frozen in liquid nitrogen after extraction, and homogenized in two cycles of 20 s at 5,500 rpm using a Precellys 24 tissue homogenator (Bertin Technologies) in 20 mM Tris buffer (pH 7.4) containing 150 mM NaCl, 1% Triton X-100, 10 mM EDTA, and Complete protease inhibitor cocktail (Roche Applied Science). Tissue extracts were then centrifuged at 12000 × *g* at 4°C and supernatants collected. Protein concentration in the supernatants was evaluated by the bicinchoninic acid technique (BCA protein assay kit, Pierce Biotechnology).

### Hormone-Induced Breast Cancers

Six-week-old female BALB/c or C57BL/6 mice underwent subcutaneous surgical implantation of 50 mg of slow-release medroxyprogesterone acetate pellets (90-day release; Innovative Research of America). 200 μl of 5 mg/ml dimethylbenzanthracene (DMBA; Sigma-Aldrich) dissolved in corn oil was administered by oral gavage six times over a period of 8 weeks. When tumors became palpable, mice received either 5.17 mg/kg MTX (intraperitoneally) in 100 μl PBS or an equivalent volume of PBS, alone or in combination with 100 mg/kg HC (intraperitoneally), 500 mg of monoclonal anti-CD4 (clone GK1.5) (intraperitoneally), and/or anti-CD8a (clone 2.43) antibodies (on the day before the onset of the treatment).

### Induction of Lung Cancer

Inhalation of 6- to 8-week-old mice with Cre recombinase-encoding adenovirus (Ad-Cre) was performed as previously reported (Rao et al., 2014). In brief, experimental animals were anesthetized with 10% ketasol/xylasol and placed on a heated pad. An Ad-Cre-$CaCl_2$ precipitate was produced by mixing 60 ml of minimal essential medium, 2.5 ml of Ad-Cre (1010 plaque-forming units $ml^{-1}$; University of Iowa Gene Transfer Vector Core) and 0.6 ml of $CaCl_2$ (1 M) for each mouse and incubated for 20 min at room temperature. One week after Ad-Cre inhalation, mice were administered 900 mg/kg HC per body weight in drinking water for 5 weeks and tumors lesion were evaluated by immunohistochemistry.

### Statistical Analysis of In Vivo Experiments

Longitudinal analysis of tumor growth data was carried out by linear mixed-effect modeling on log pre-processed tumor sizes. Wald tests were used to compute p values by testing jointly that both tumor growth slopes and intercepts (on a log scale) were the same between treatment groups of interest (Demidenko, 2006; Sugar et al., 2012). At a single time point, the effect of treatment was estimated by linear modeling. p Values were adjusted according to the Holm method from all pairwise comparisons of interest. For graphing, tumor growth data are represented on the untransformed original scale in three forms: (1) explicit curves from all measurements of each mouse; (2) group-averaged tumor size alongside its SEM computed at each time point; (3) overlay of single data points and the classical box-and-whiskers plot at a selected sampling point. For mice euthanized before the selected sampling point, the last measure was retained.

Additional procedural details are available in Supplemental Experimental Procedures.

## Supplementary Material

Refer to Web version on PubMed Central for supplementary material.

## Acknowledgments

G.K. and L.Z. are supported by the Ligue Nationale contre le Cancer (Equipes labellisées), Site de Recherche Intégrée sur le Cancer (IRIC) Socrates, the ISREC Foundation, Agence Nationale pour la Recherche (ANR AUTOPH, ANR Emergence), the European Commission (ArtForce), a European Research Council Advanced Investigator Grant (to G.K.), the Foundation pour la Recherche M&eacute dicale (FRM), the Institute National du Cancer (INCa), the Foundation de France, Cancéropole Ile-de-France, the Fondation Bettencourt-Schueller, the Lab

ExImmuno-Oncology, and the Paris Alliance of Cancer Research Institutes. J.M.P. is supported by EU network grants Apo-Sys ApoSys and InflaCare, an advanced ERC grant, and an Era of Hope/DoD Innovator Award. F.M. is grateful to the FWF for grants LIPOTOX, I1000, P23490-B12, and P24381-B20, and the BMWFW for grant Unconventional research. F.D.V. is supported by grants from the AIRC (no. IG5354), Telethon (no. GGP06070), ERA-NET Neuron “Nanostroke”, the Ministry of Health of Italy (no. RF-2011-02348435), the Italian Ministry of Education, University and Research (no. RBAP11FXBC_001), and funds from the University of Ferrara. B.L. is supported by NIH grants RO1CA109618 and U19 AI109725, and Cancer Prevention and Research Institute of Texas grant RP120718. E.E.B. is supported by Cancéropôle Ile-de-France. We thank Prof. Eric Tartour and Dr. Johannes Ludger for TC1-specific HPV16-E7 tetramer. We are grateful to Dr. Lorenzo Galluzzi for the extensive proofreading of manuscript and figures.

## References

Bindea G, Mlecnik B, Tosolini M, Kirilovsky A, Waldner M, Obenauf AC, Angell H, Fredriksen T, Lafontaine L, Berger A, et al. Spatiotemporal dynamics of intratumoral immune cells reveal the immune landscape in human cancer. Immunity. 2013; 39:782–795. [PubMed: 24138885]

Casagrande DS, Rosa DD, Umpierre D, Sarmento RA, Rodrigues CG, Schaan BD. Incidence of cancer following bariatric surgery: systematic review and meta-analysis. Obes Surg. 2014; 24:1499–1509. [PubMed: 24817500]

Cheng CW, Adams GB, Perin L, Wei M, Zhou X, Lam BS, Da Sacco S, Mirisola M, Quinn DI, Dorff TB, et al. Prolonged fasting reduces IGF-1/PKA to promote hematopoietic-stem-cell-based regeneration and reverse immunosuppression. Cell Stem Cell. 2014; 14:810–823. [PubMed: 24905167]

Chuah LO, Yeap SK, Ho WY, Beh BK, Alitheen NB. In vitro and in vivo toxicity of garcinia or hydroxycitric acid: a review. Evid Based Complement Alternat Med. 2012; 2012:197920. [PubMed: 22924054]

Demidenko E. The assessment of tumour response to treatment. J R Stat Soc Ser C. 2006; 55:365–377.

Eisenberg T, Knauer H, Schauer A, Buttner S, Ruckenstuhl C, Carmona-Gutierrez D, Ring J, Schroeder S, Magnes C, Antonacci L, et al. Induction of autophagy by spermidine promotes longevity. Nat Cell Biol. 2009; 11:1305–1314. [PubMed: 19801973]

Galluzzi L, Buque A, Kepp O, Zitvogel L, Kroemer G. Immunological effects of conventional chemotherapy and targeted anticancer agents. Cancer Cell. 2015a; 28:690–714. [PubMed: 26678337]

Galluzzi L, Pietrocola F, Bravo-San Pedro JM, Amaravadi RK, Baehrecke EH, Cecconi F, Codogno P, Debnath J, Gewirtz DA, Karantza V, et al. Autophagy in malignant transformation and cancer progression. EMBO J. 2015b; 34:856–880. [PubMed: 25712477]

Gilbert CA, Slingerland JM. Cytokines, obesity, and cancer: new insights on mechanisms linking obesity to cancer risk and progression. Annu Rev Med. 2013; 64:45–57. [PubMed: 23121183]

Guo JY, Xia B, White E. Autophagy-mediated tumor promotion. Cell. 2013; 155:1216–1219. [PubMed: 24315093]

Harrison DE, Strong R, Sharp ZD, Nelson JF, Astle CM, Flurkey K, Nadon NL, Wilkinson JE, Frenkel K, Carter CS, et al. Rapamycin fed late in life extends lifespan in genetically heterogeneous mice. Nature. 2009; 460:392–395. [PubMed: 19587680]

Jiang P, Mizushima N. Autophagy and human diseases. Cell Res. 2014; 24:69–79. [PubMed: 24323045]

Kalaany NY, Sabatini DM. Tumours with PI3K activation are resistant to dietary restriction. Nature. 2009; 458:725–731. [PubMed: 19279572]

Kepp O, Senovilla L, Kroemer G. Immunogenic cell death inducers as anticancer agents. Oncotarget. 2014; 5:5190–5191. [PubMed: 25114034]

Kibe R, Kurihara S, Sakai Y, Suzuki H, Ooga T, Sawaki E, Muramatsu K, Nakamura A, Yamashita A, Kitada Y, et al. Upregulation of colonic luminal polyamines produced by intestinal microbiota delays senescence in mice. Sci Rep. 2014; 4:4548. [PubMed: 24686447]

Klionsky DJ, Abdalla FC, Abeliovich H, Abraham RT, Acevedo-Arozena A, Adeli K, Agholme L, Agnello M, Agostinis P, Aguirre-Ghiso JA, et al. Guidelines for the use and interpretation of assays for monitoring autophagy. Autophagy. 2012; 8:445–544. [PubMed: 22966490]

Ko A, Kanehisa A, Martins I, Senovilla L, Chargari C, Dugue D, Marino G, Kepp O, Michaud M, Perfettini JL, et al. Autophagy inhibition radiosensitizes in vitro, yet reduces radioresponses in vivo due to deficient immunogenic signalling. Cell Death Differ. 2014; 21:92–99. [PubMed: 24037090]

Lahl K, Loddenkemper C, Drouin C, Freyer J, Arnason J, Eberl G, Hamann A, Wagner H, Huehn J, Sparwasser T. Selective depletion of Foxp3+ regulatory T cells induces a scurfy-like disease. J Exp Med. 2007; 204:57–63. [PubMed: 17200412]

Lee C, Longo VD. Fasting vs dietary restriction in cellular protection and cancer treatment: from model organisms to patients. Oncogene. 2011; 30:3305–3316. [PubMed: 21516129]

Lee C, Raffaghello L, Brandhorst S, Safdie FM, Bianchi G, Martin-Montalvo A, Pistoia V, Wei M, Hwang S, Merlino A, et al. Fasting cycles retard growth of tumors and sensitize a range of cancer cell types to chemotherapy. Sci Transl Med. 2012; 4:124ra127.

Levine BL, June CH. Perspective: assembly line immunotherapy. Nature. 2013; 498:S17. [PubMed: 23803946]

Levine B, Packer M, Codogno P. Development of autophagy inducers in clinical medicine. J Clin Invest. 2015; 125:14–24. [PubMed: 25654546]

Loi S, Pommey S, Haibe-Kains B, Beavis PA, Darcy PK, Smyth MJ, Stagg J. CD73 promotes anthracycline resistance and poor prognosis in triple negative breast cancer. Proc Natl Acad Sci U S A. 2013a; 110:11091–11096. [PubMed: 23776241]

Ma Y, Adjemian S, Mattarollo SR, Yamazaki T, Aymeric L, Yang H, Portela Catani JP, Hannani D, Duret H, Steegh K, et al. Anticancer chemotherapy-induced intratumoral recruitment and differentiation of antigen-presenting cells. Immunity. 2013; 38:729–741. [PubMed: 23562161]

Madeo F, Pietrocola F, Eisenberg T, Kroemer G. Caloric restriction mimetics: towards a molecular definition. Nat Rev Drug Discov. 2014; 13:727–740. [PubMed: 25212602]

Makarem N, Chandran U, Bandera EV, Parekh N. Dietary fat in breast cancer survival. Annu Rev Nutr. 2013; 33:319–348. [PubMed: 23701588]

Marino G, Pietrocola F, Eisenberg T, Kong Y, Malik SA, Andryushkova A, Schroeder S, Pendl T, Harger A, Niso-Santano M, et al. Regulation of autophagy by cytosolic acetyl-coenzyme A. Mol Cell. 2014; 53:710–725. [PubMed: 24560926]

Martins I, Wang Y, Michaud M, Ma Y, Sukkurwala AQ, Shen S, Kepp O, Metivier D, Galluzzi L, Perfettini JL, et al. Molecular mechanisms of ATP secretion during immunogenic cell death. Cell Death Differ. 2014; 21:79–91. [PubMed: 23852373]

McNally A, Hill GR, Sparwasser T, Thomas R, Steptoe RJ. CD4+CD25+ regulatory T cells control CD8+ T-cell effector differentiation by modulating IL-2 homeostasis. Proc Natl Acad Sci U S A. 2011; 108:7529–7534. [PubMed: 21502514]

Michaud M, Martins I, Sukkurwala AQ, Adjemian S, Ma Y, Pellegatti P, Shen S, Kepp O, Scoazec M, Mignot G, et al. Autophagy-depen-dent anticancer immune responses induced by chemotherapeutic agents in mice. Science. 2011; 334:1573–1577. [PubMed: 22174255]

Michaud M, Xie X, Bravo-San Pedro JM, Zitvogel L, White E, Kroemer G. An autophagy-dependent anticancer immune response determines the efficacy of melanoma chemotherapy. Oncoimmunology. 2014; 3:e944047. [PubMed: 25610726]

Mizushima N, Yamamoto A, Matsui M, Yoshimori T, Ohsumi Y. In vivo analysis of autophagy in response to nutrient starvation using transgenic mice expressing a fluorescent autophagosome marker. Mol Biol Cell. 2004; 15:1101–1111. [PubMed: 14699058]

Mizushima N, Levine B, Cuervo AM, Klionsky DJ. Autophagy fights disease through cellular self-digestion. Nature. 2008; 451:1069–1075. [PubMed: 18305538]

Morselli E, Marino G, Bennetzen MV, Eisenberg T, Megalou E, Schroeder S, Cabrera S, Benit P, Rustin P, Criollo A, et al. Spermidine and resveratrol induce autophagy by distinct pathways converging on the acetylproteome. J Cell Biol. 2011; 192:615–629. [PubMed: 21339330]

Obeid M, Tesniere A, Ghiringhelli F, Fimia GM, Apetoh L, Perfettini JL, Castedo M, Mignot G, Panaretakis T, Casares N, et al. Calreticulin exposure dictates the immunogenicity of cancer cell death. Nat Med. 2007; 13:54–61. [PubMed: 17187072]

Onakpoya I, Hung SK, Perry R, Wider B, Ernst E. The use of Garcinia extract (hydroxycitric acid) as a weight loss supplement: a systematic review and meta-analysis of randomised clinical trials. J Obes. 2011; 2011:509038. [PubMed: 21197150]

Pellegatti P, Raffaghello L, Bianchi G, Piccardi F, Pistoia V, Di Virgilio F. Increased level of extracellular ATP at tumor sites: in vivo imaging with plasma membrane luciferase. PLoS One. 2008; 3:e2599. [PubMed: 18612415]

Pietrocola F, Lachkar S, Enot DP, Niso-Santano M, Bravo-San Pedro JM, Sica V, Izzo V, Maiuri MC, Madeo F, Marino G, Kroemer G. Spermidine induces autophagy by inhibiting the acetyltransferase EP300. Cell Death Differ. 2015; 22:509–516. [PubMed: 25526088]

Rao S, Tortola L, Perlot T, Wirnsberger G, Novatchkova M, Nitsch R, Sykacek P, Frank L, Schramek D, Komnenovic V, et al. A dual role for autophagy in a murine model of lung cancer. Nat Commun. 2014; 5:3056. [PubMed: 24445999]

Rubinsztein DC, Codogno P, Levine B. Autophagy modulation as a potential therapeutic target for diverse diseases. Nat Rev Drug Discov. 2012; 11:709–730. [PubMed: 22935804]

Shoji-Kawata S, Sumpter R, Leveno M, Campbell GR, Zou Z, Kinch L, Wilkins AD, Sun Q, Pallauf K, MacDuff D, et al. Identification of a candidate therapeutic autophagy-inducing peptide. Nature. 2013; 494:201–206. [PubMed: 23364696]

Sistigu A, Yamazaki T, Vacchelli E, Chaba K, Enot DP, Adam J, Vitale I, Goubar A, Baracco EE, Remedios C, et al. Cancer cell-autonomous contribution of type I interferon signaling to the efficacy of chemotherapy. Nat Med. 2014; 20:1301–1309. [PubMed: 25344738]

Stagg J, Divisekera U, Duret H, Sparwasser T, Teng MW, Darcy PK, Smyth MJ. CD73-deficient mice have increased antitumor immunity and are resistant to experimental metastasis. Cancer Res. 2011; 71:2892–2900. [PubMed: 21292811]

Strong R, Miller RA, Astle CM, Floyd RA, Flurkey K, Hensley KL, Javors MA, Leeuwenburgh C, Nelson JF, Ongini E, et al. Nordihydroguaiaretic acid and aspirin increase lifespan of genetically heterogeneous male mice. Aging Cell. 2008; 7:641–650. [PubMed: 18631321]

Sugar E, Pascoe AJ, Azad N. Reporting of preclinical tumorgraft cancer therapeutic studies. Cancer Biol Ther. 2012; 13:1262–1268. [PubMed: 22895077]

Tee MC, Cao Y, Warnock GL, Hu FB, Chavarro JE. Effect of bariatric surgery on oncologic outcomes: a systematic review and meta-analysis. Surg Endosc. 2013; 27:4449–4456. [PubMed: 23949484]

Teng MW, Ngiow SF, von Scheidt B, McLaughlin N, Sparwasser T, Smyth MJ. Conditional regulatory T-cell depletion releases adaptive immunity preventing carcinogenesis and suppressing established tumor growth. Cancer Res. 2010; 70:7800–7809. [PubMed: 20924111]

Tesniere A, Schlemmer F, Boige V, Kepp O, Martins I, Ghiringhelli F, Aymeric L, Michaud M, Apetoh L, Barault L, et al. Immunogenic death of colon cancer cells treated with oxaliplatin. Oncogene. 2010; 29:482–491. [PubMed: 19881547]

Uhl M, Kepp O, Jusforgues-Saklani H, Vicencio JM, Kroemer G, Albert ML. Autophagy within the antigen donor cell facilitates efficient antigen cross-priming of virus-specific CD8+ T cells. Cell Death Differ. 2009; 16:991–1005. [PubMed: 19229247]

White E. The role for autophagy in cancer. J Clin Invest. 2015; 125:42–46. [PubMed: 25654549]

Yamaguchi T, Hirota K, Nagahama K, Ohkawa K, Takahashi T, Nomura T, Sakaguchi S. Control of immune responses by antigen-specific regulatory T cells expressing the folate receptor. Immunity. 2007; 27:145–159. [PubMed: 17613255]

Zitvogel L, Galluzzi L, Smyth MJ, Kroemer G. Mechanism of action of conventional and targeted anticancer therapies: reinstating immuno-surveillance. Immunity. 2013; 39:74–88. [PubMed: 23890065]

## Highlights

- Short-term fasting improves anticancer chemotherapy
- Treatment with caloric restriction mimetics (CRMs) inhibits tumor growth in vivo
- CRMs trigger an autophagy-dependent anticancer immune response
- CRMs deplete regulatory T Cells from tumor bed

## Significance

Fasting can improve the efficacy of anticancer chemotherapy. We show here that this effect involves induction of autophagy in malignant cells, as well as an anticancer immune response. Fasting can be replaced by the administration of caloric restriction mimetics (CRMs), which—without causing weight loss—improve the efficacy of chemotherapy as well. The tumor growth-inhibitory effects of hydroxycitrate were epistatic to the inhibition of regulatory T cells. Altogether, our results reveal a common mechanism for the cancer protective properties of CRMs and point to the possibility of stimulating anticancer immune responses by inducing autophagy with well-tolerable CRMs in vivo.

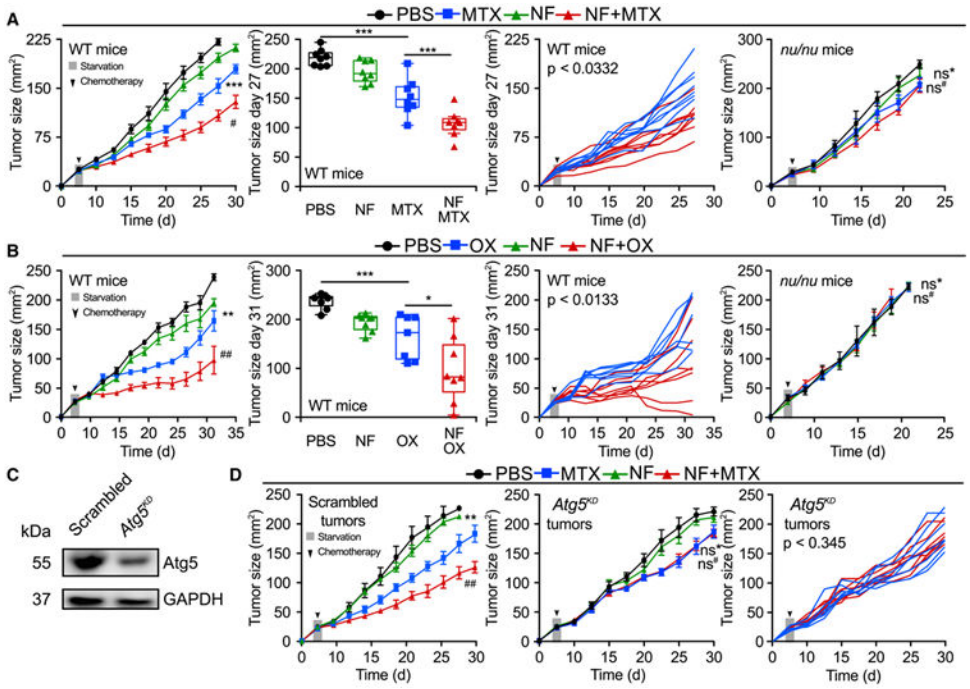


**Figure 1. Fasting Improves the Efficacy of Chemotherapy in an Immune System- and Autophagy-Dependent Fashion**

(A and B) Immune system-dependent effects of starvation. Wild-type (WT) immunocompetent C57BL/6 and athymic mice (*nu*/*nu*) mice were inoculated subcutaneously with murine fibrosarcoma MCA205 cells. When tumors became palpable, mice were fed ad libitum or underwent 48 hr fasting (NF, nutrient free) and received intraperitoneal chemotherapy with mitoxantrone (MTX) (A) or oxaliplatin (OX) (B), or an equivalent volume of PBS (PBS). From left to right: (1) average (±SEM) tumor growth curves of WT mice subjected to 48 hr starvation alone or in combination with MTX or OX from one representative experiment of two with at least seven mice per group; (2) tumor size distribution at day 27 (MTX) or day 31 (OX) of data shown in (1); (3) individual growth curves from mice treated with MTX or OX alone or combined with fasting of data shown in (1); (4) averaged (±SEM) tumor growth curves from immunodeficient *nu*/*nu* mice subjected to 48 hr starvation alone or in combination with MTX or OX from one representative experiment of two with at least five mice per group. For *nu*/*nu* mice, PBS and MTX groups are shared with experiments depicted in Figures 4B–4D.

(C and D) Autophagy deficiency impairs starvation-mediated improvement in anthracycline-based therapy. (C) Immunoblot showing effective knockdown of *Atg5* in murine MCA205 fibrosarcoma cells. (D) WT immunocompetent C57BL/6 mice were inoculated subcutaneously with autophagy-competent control cells expressing a scrambled control shRNA (left panel) or *Atg5KD* MCA205 cells (middle and right panels). When tumor became palpable, they were treated as in (A). Data are shown as averaged (±SEM) tumor growth curves of at least five mice per group from one representative experiment of two (left/middle panels) or as individual curves from mice treated with MTX alone or combined with fasting (right panel). Statistical analysis was performed by linear mixed-effect modeling (over the whole time course) and linear modeling (at a single time point). ***p <

0.001, **p < 0.01, *p < 0.05 (PBS versus MTX or OX); ##p < 0.01, #p < 0.05 (MTX versus MTX + NF or OX versus NF + OX); ns, not significant. For a comprehensive account of all comparisons, see also Tables S1 and S2.

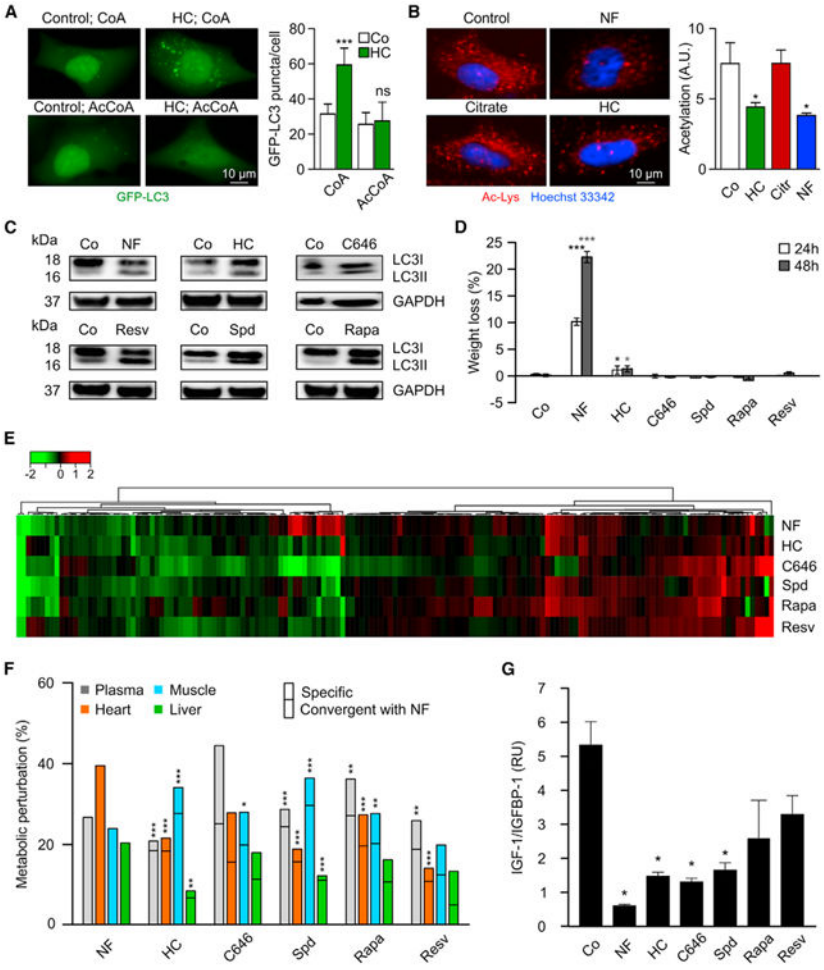


**Figure 2. Autophagy Induction and Metabolic Effects of Hydroxycitrate and Other Caloric Restriction Mimetics**

(A) Inhibition of hydroxycitrate (HC)-induced autophagy by microinjection of acetyl coenzyme A (AcCoA) but not coenzyme A (CoA). U2OS cells stably expressing the autophagic marker GFP-LC3 were treated with HC for 6 hr and injected with 10 μM AcCoA or CoA. Representative pictures (left panel) and quantification (right panel, mean ± SD, n = 3).

(B) Deacetylation of cytoplasmic proteins in response to 20 mM HC or cultured in a nutrient-free condition (NF). Representative pictures (left panel) and quantification (right panel, mean ± SEM, n = 3).

(C) LC3I to LC3II conversion induced by starvation (48 hr) or short-term intraperitoneal injection of HC, C646, resveratrol (Resv), spermidine (Spd), or rapamycin (Rapa) in liver. For the characterization of the mode of action of HC, see Figure S1.

(D) Weight loss (mean ± SD, n = 5) induced by 24 and 48 hr starvation or administration of the indicated agents in C57BL/6 mice.

(E) Heatmap depicting $\log_2$ fold changes to the control of metabolite signals found significantly altered in the plasma of mice after 48 hr starvation or after two injections of corresponding caloric restriction mimetics (CRMs). For other organs, see Figure S2. For the complete list of metabolites, see Table S3.

(F) Summary of significant ($p < 0.05$) metabolic alterations elicited by 48 hr of starvation or CRMs in different mouse tissues and plasma of data shown in (E).CRMs-induced alterations were considered as convergent with starvation when they had the same sign.
(G) Effect of starvation and CRMs on plasma levels of insulin growth factor 1 (IGF-1) and IGF binding protein 1 (IGFBP1). Results are depicted as mean ± SEM (n = 3, two experiments).
Statistical analysis was performed by Student's t test in comparison with the control condition (B, D, and G) and by Fisher's exact test to compare convergence incidences with those in NF (F). ***$p < 0.001$, **$p < 0.01$, *$p < 0.05$; ns, not significant.

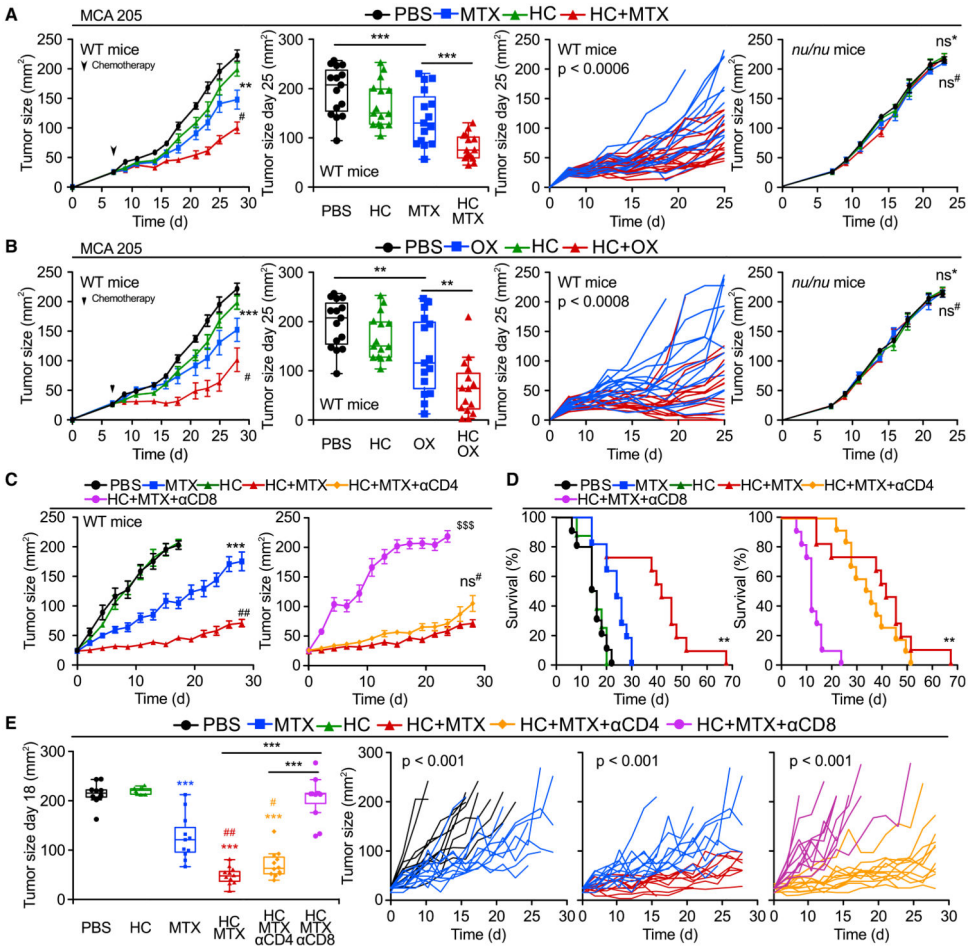


**Figure 3. Hydroxycitrate Improves Antitumor Immunity in an Immune System-Dependent Manner**

(A and B) Immune-dependent effects of hydroxycitrate (HC) on transplanted tumors. Wild-type (WT) immunocompetent C57Bl/6 and athymic mice (*nu*/*nu*) mice were inoculated subcutaneously with murine fibrosarcoma MCA205 cells. When tumors became palpable, mice were treated with HC in drinking water and received one intraperitoneal injection of chemotherapy with mitoxantrone (MTX) (A), oxaliplatin (OX) (B) on the second day, or PBS (PBS)as a vehicle control. From left to right: (1) averaged (± SEM, pool of two independent experiments, at least seven mice per group sharing PBS and HC groups) growth curves from WT mice subjected to HC administration alone or in combination with MTX or OX; (2) tumor size distributions at day 25 (MTX and OX) of data shown in(1); (3) individual tumor growth curves of mice treated with MTX or OX alone or in combination with HC of data shown in(1); (4) averaged (±SEM, one representative experiment of two with at least five mice per group) growth curves from immunodeficient *nu*/*nu* mice subjected to HC treatment in drinking water alone or in combination with MTX or OX.

(C–E) Immune system-dependent effects of HC on hormone-induced breast cancers. Immunocompetent BALB/c mice bearing palpable hormone-induced mammary cancers received intraperitoneal chemotherapy with MTX and/or 100 mg/kg HC, alone or together with antibodies depleting $CD8^+$ or $CD4^+$ T cells. Data are shown as: (C) averaged (± SEM,

two independent experiments, at least eight mice per group); (D) Kaplan-Meier curves with death or tumor size exceeding 200 $mm^2$ as endpoint; (E) distributions across treatment groups at day 18 and explicitly graphing up to 28 days post intraperitoneal treatment. Note that PBS curve in (C) ends at day 18 since averaged (but not single mice) tumor size of the group reached ethical limits.

Statistical analyses were conducted by linear mixed-effect modeling (over the whole time course), linear modeling (at a single time point) and log-rank test (survival curves). ***$p < 0.001$, **$p < 0.01$ (comparisons with PBS or explicitly denoted by a segment); $^{\#\#}p < 0.01$, $^{\#}p < 0.05$ (comparisons with chemotherapy alone); $^{\$\$\$}p < 0.001$ (HC + MTX versus HC + MTX + αCD8); ns, not significant. For a detailed account of all comparisons, see Tables S1 and S2. For HC effects on autophagy in tumors and additional models of transplantable cancers, see Figures S3 and S4.

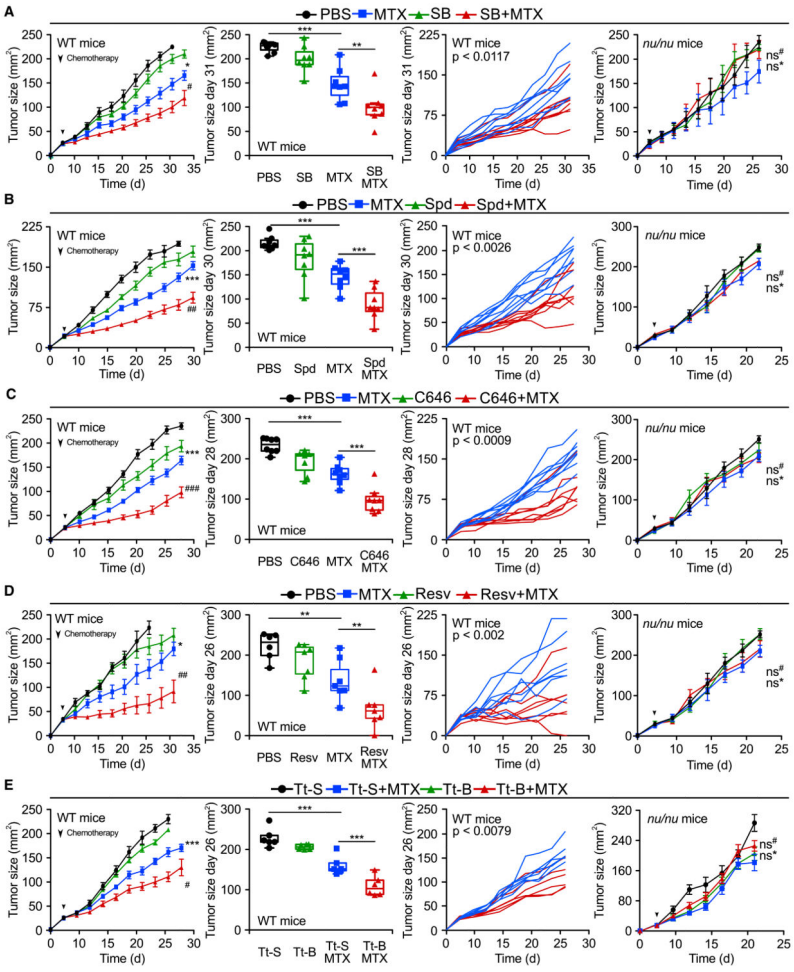


**Figure 4. Multiple Autophagy Inducers Reduce Tumor Growth via an Immunological Mechanism**

(A–E) Wild-type (WT) immunocompetent C57BL/6 and athymic mice (*nu*/*nu*) mice were inoculated subcutaneously with murine fibrosarcoma MCA205 cells. When tumors became palpable, mice received systemic intraperitoneal injection of the ATP citrate lyase inhibitor SB204990 (SB) (A), the natural EP300 acetyltransferase inhibitor spermidine (Spd) (B), the EP300 inhibitor C646 (C), Resveratrol (Resv) (D), and the autophagy-inducing peptide Tt-B or its mutant control Tt-S (E), alone or together with mitoxantrone (MTX). Results (averaged ±SEM tumor growth curves) are plotted and statistical calculations performed as previously described.

**p < 0.01, ***p < 0.001; *ns, not significant (PBS versus chemotherapy); $^{\#}p < 0.05$, $^{\#\#}p < 0.01$, $^{\#\#\#}p < 0.001$ (chemotherapy versus CRMs + chemotherapy). For other statistical comparisons, see Tables S1 and S2. For additional evidence of immune mechanisms involved in the anticancer effects of CRMs, see Figure S4. For the characterization of the pro-autophagic effects of peptide Tt-B, see Figure S5.

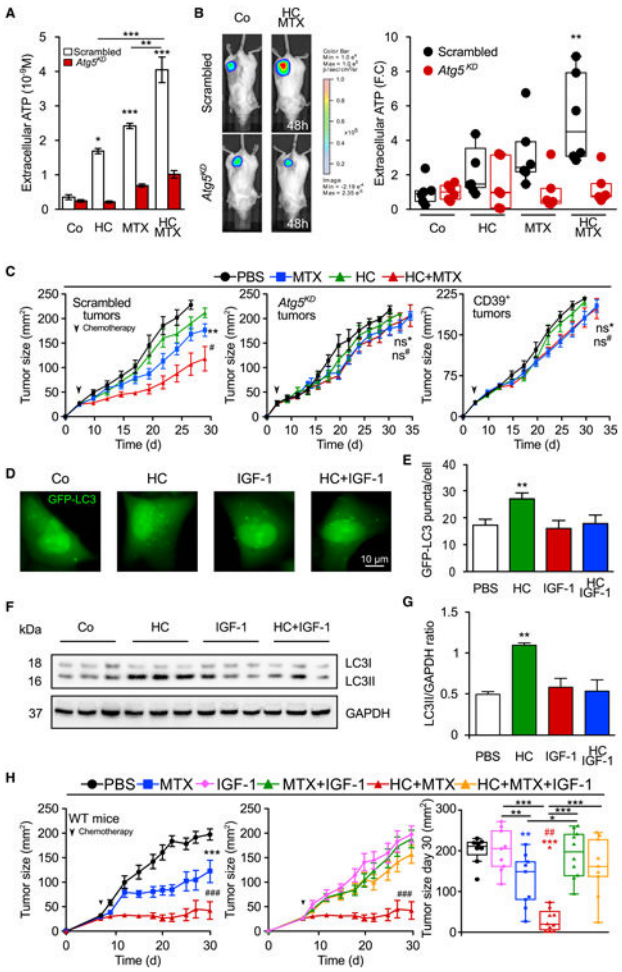


**Figure 5. Autophagy and ATP-Dependent Improvement of Anticancer Chemotherapy by Hydroxycitrate**

(A) Autophagy-dependent release of ATP in vitro. ATP concentration (mean ± SEM, n = 7, pooled from two experiments) was measured in the supernatants of autophagy-competent or *Atg5*$^{KD}$ *CT26* cells treated with 20 mM hydroxycitrate (HC) and/or 2 μM mitoxantrone (MTX).

(B) Autophagy-dependent release of ATP in vivo. Autophagy-competent or *Atg5*$^{KD}$ CT26 colorectal cancers expressing a luciferase variant detecting extracellular ATP were treated with MTX and/or HC, and ATP release was monitored until 48 hr post chemotherapy. Representative images (left panel) and corresponding box plots of quantification (right panel) expressed as fold change of photon flux ratio.

(C) Requirement of autophagy and extracellular ATP for the anti cancer effects of the MTX/HC combination. Tumor growth curves (mean ± SEM) from C57BL/6 mice bearing autophagy-competent or autophagy-deficient (*Atg5*$^{KD}$) MCA205 tumors or MCA205 tumors or over expressing a CD39 transgene (CD39$^{+}$) received MTX and/or HC.

(D) Inhibition of HC-induced autophagy by IGF-1. U2OS cells stably expressing the autophagic marker GFP-LC3 were treated with HC alone or in combination with 10 mM insulin growth factor 1 (IGF-1).

(E–G) (E) Autophagy was measured by assessing the abundance of GFP-LC3 puncta per cell (in the presence of BafA1) and quantified in (F, mean ± SEM, n = 3). WT immunocompetent C57BL/6 mice bearing MCA205-derived tumors were treated with HC alone or in combination with recombinant IGF-1. Autophagy was assessed by immunoblotting in the tumor (F) and quantified in (G, mean ± SEM, n = 3).
(H) Reversal of the therapeutic effect of HC by IGF-1. WT immunocompetent C57BL/6 mice were inoculated subcutaneously with murine fibrosarcoma MCA205 cells and tumors were treated withHCand/or MTX, aloneor combined with intraperitoneal injectionsof recombinant IGF-1 protein (averaged ±SEM tumor growth curves).
Data were analyzed by ANOVA for multiple comparisons (A and B), unpaired Student's t test (E and G), linear mixed-effect modeling (C and H), and linear modeling (H). Levels of significance: ***$p < 0.001$, **$p < 0.01$, *$p < 0.05$ (comparisons with Co/PBS unless indicated by a segment); $^{###}p < 0.001$, $^{#}p < 0.05$ (comparisons between chemotherapy and chemotherapy + CRM); ns, not significant. For the indication of all statistical comparisons of (C) and (H), see Tables S1 and S2.

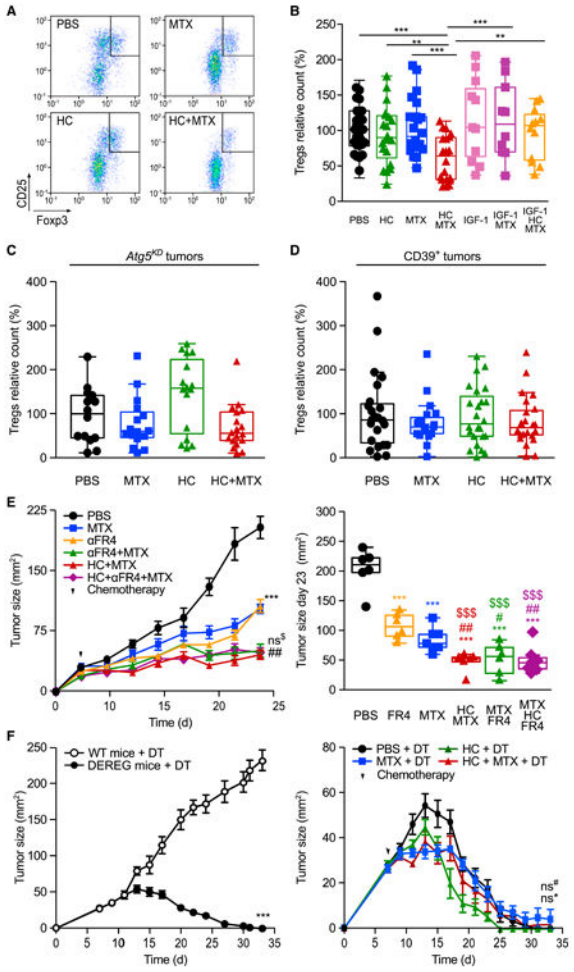


**Figure 6. Autophagy and ATP-Dependent Depletion of Intratumoral Tregs by Hydroxycitrate**

(A) Representative fluorescence-activated cell sorting profiles and quantification of $CD4^+CD25^+Foxp3^+$ cells in the tumor infiltrate from cancers treated with mitoxantrone (MTX) and/or hydroxycitrate (HC) 11 days post chemotherapy.

(B) Effects of MTX, HC, and insulin growth factor 1 (IGF-1) on the frequency of tumor-infiltrating $CD4^+CD25^+Foxp3^+$ cells.

(C and D) Effects of MTX and HC on the frequency of $CD4^+CD25^+Foxp3^+$ Tregs infiltrating autophagy-deficient $Atg5^{KD}$ (C) or CD39-overexpressing (D) tumors. In (B–D), data are relative to the control (PBS) group of each experiment each dot represents a distinct tumor.

(E and F) Regulatory T cell (Treg) depletion and HC administration similarly improve the effect of MTX. (E) Wild-type (WT) immunocompetent C57BL/6 mice were inoculated subcutaneously with MCA205 cells. When the tumor became palpable, mice received MTX, 100 mg/kg intraperitoneal HC, and/or anti-FR4 antibody. Averaged (±SEM, one experiment involving six mice per group) tumor sizes are reported for the entire duration of the experiment (left panel) together with the tumor size distributions at day 23 (right panel). (F) C57BL/6-Tg (Foxp3-DTR/EGFP) DEREG (DEpletion of REGulatory T cells) transgenic mice and their WT lit-termates were inoculated subcutaneously with MCA205 cells. When

tumors became palpable, mice were injected intraperitoneally daily with 1 μg/kg diphtheria toxin (DT) for 15 days. DEREG mice were administered with HC in drinking water. At day 2 post DT and HC administration, DEREG mice received chemotherapy with MTX or PBS. Results are shown as means ± SEM (at least eight mice per group).

Data were analyzed by ANOVA for multiple comparisons (B–D), linear mixed-effect modeling (E, left panel, and F), and linear modeling (E, right panel). Levels of significance: ***$p < 0.001$, **$p < 0.01$, *$p < 0.05$ (comparisons with PBS); $^{\#\#}p < 0.01$, (comparisons between MTX and MTX combinations); $^{\$\$\$}p < 0.001$ (comparisons with anti-FR4 antibody); ns, not significant. For all comparisons in (B–F), see Tables S1 and S2. For additional evidence for the involvement of extracellular ATP metabolism and Treg depletion in the anticancer effects of HC, see Figure S6.

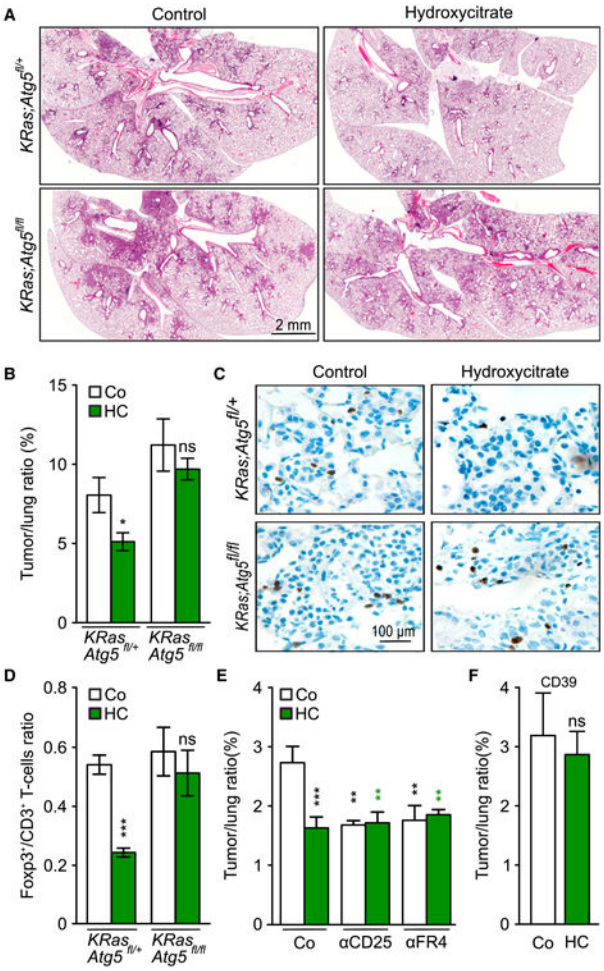


**Figure 7. Hydroxycitrate Improves Antitumor Immunity in an Autophagy-Dependent Manner**

(A and B) Hydroxycitrate (HC) reduces tumor size and lesions in KRas-induced lung cancer in *KRas*;*Atg5*$^{fl/+}$ mice but not in *KRas*;*Atg5*$^{fl/fl}$ littermates. (A) H&E staining of representative histological sections after Cre recombinase-encoding adenovirus (Ad-Cre) inhalation and after 5 weeks HC administration in drinking water. (B) Quantification of data depicted in (A). Results are expressed as means ± SEM from three different experiments.

(C and D) HC reduces $CD3^+Foxp3^+$ Tregs in tumor beds of *KRas*;*Atg5*$^{fl/+}$ mice but not *KRas*;*Atg5*$^{fl/fl}$ littermates. Representative histological sections of $Foxp3^+$ stained T cells after 5 weeks of HC administration (C) and corresponding quantification (D) (mean ± SEM, three independent experiments).

(E) Epistatic analysis demonstrating that depletion of Tregs by administration of aFR4 or aCD25 antibodies reproduces the antitumor effect of HC.Results are illustrated as means ± SEM from threeexperiments.

(F) Antitumor effects of HC in KRas-driven lungcancer is abrogated upon Cre-recombinase-induced expression of a CD39 transgene. 6- to 8-week-old *CD39*; *KRas*; *Atg5*$^{fl/+}$ mice were treated byinhalation of Cre recombinase-encoding adenovirus(Ad-Cre). One week after recovery, mice were administered HC for 5 weeks. Results are shown asmeans ± SEM.

Comparisons with the control group or untreated tumors were done by Student's t test. ***p < 0.001, **p < 0.01, *p < 0.05; ns, not significant. For additional immunohistochemical characterization of HC effects on KRas-induced tumors, see Figure S7.